Microphotoluminescence and Microphotoreflectance Analyses of CO_2 Laser Rapid-Thermal-Annealed SiO_x Surface With Buried Si Nanocrystals

Gong-Ru Lin, *Senior Member, IEEE*, Chun-Jung Lin, Li-Jen Chou, and Yu-Lun Chueh

***Abstract*—The optical properties of a SiO_x film rapid-thermal-annealed (RTA) by CO_2 laser are primarily investigated. The microphotoluminescence (μ-PL) and high-resolution transmission electron microscopy (HRTEM) analyses indicate that the precipitation of random-oriented Si nanocrystals can be initiated when laser intensity ($P_{\rm laser}$) is larger than 4.5 kW/cm^2. At $P_{\rm laser}$ of 6 kW/cm^2, the Si nanocrystal exhibits a largest diameter of 8 nm and a highest density of 4.5×10^{16} cm^{-3}, which emits strong PL at 790–825 nm. The microphotoreflectance of the CO_2 laser RTA SiO_x film reveals a volume density product dependent refractive index increasing from 1.57 to 1.87 as $P_{\rm laser}$ increases from 1.5 to 7.5 kW/cm^2. Nonetheless, the laser ablation of the SiO_x film occurs with a linear ablation slope of 35 nm/kW/cm^2 at beyond 7.5 kW/cm^2, which terminates the enlargement of Si nanocrystals, degrades the near-infrared PL, and slightly reduces the refractive index of the CO_2 laser RTA SiO_x film.**

***Index Terms*—CO_2 laser annealing, microphotoluminescence, nanotechnology, Si nanocrystal, SiO_x.**

I. Introduction

THE CO_2 LASER based zone annealing (or zone drawing) technique has previously emerged to modify the morphology or structural properties of different materials including polymers [1], [2], metallic thin films [3]–[5], superconductors [6], and dielectrics [7] etc. Particularly, such a laser heating process was also found to initiate the recrystallization and sintering of ceramic powders [8], or to enhance the surface crystallinity and the specific phase of an optical nonlinear crystal (beta-BBO) [9]. Optical microscopy has shown that the crystallite surface exhibits same morphology as those observed after traditional furnace processing; however, the effect of CO_2 laser annealing on the growth rate and the crystallite size is more pronounced. Not long ago, the CO_2 laser annealing was primarily employed to improve the properties of a liquid-phase deposited, fluorinated silicon oxide film, which helps to concentrate the fluorinated silicon oxide film and reduce the effective surface charge density caused by surface defect states [7]. Nonetheless, the CO_2 laser annealing induced modifications are intensity ($P_{\rm laser}$) dependent and usually becomes prominent at $P_{\rm laser} > 10$ kW/cm^2. Recently, the high-temperature (> 1000 °C) furnace annealing is employed to precipitate the Si nanocrystals in SiO_2 film [10]. However, such a high-temperature heat treatment could seriously damage the whole integrated circuits (ICs) on the same Si wafer, which constrains the monolithic integration of the Si nanocrystal doped SiO_x layer with the Si-based ICs. Owing to the large absorption coefficient as high as 1.2×10^3 cm^{-1} of the oxide material at wavelength of 10.6 μm, a CO_2 laser annealing of SiO_x film on quartz substrate is investigated for the first time. In this paper, the optical properties and the size/density of localized precipitated Si nanocrystals embedded in the CO_2-laser rapid-thermal-annealed (RTA) SiO_x film are analyzed by high-resolution transmission electron microscopy (HRTEM), microphotoluminescence (μ-PL), and microphotoreflectance (μ-PR).

II. Experimental

The 280-nm-thick SiO_x films were deposited on both-side-polished quartz substrates by using high-density plasma enhanced chemical vapor deposition (PECVD) with a gas mixture of SiH_4 and N_2O. The substrate temperature was kept at 150 °C for 15 min to balance the temperature of the quartz substrate before deposition. The fluence ratio of SiH_4 to N_2O, the rf power, and the reaction gas pressure were 1 : 6, 50 W, and 120 mtorr, respectively. Afterwards, the CO_2 laser RTA was performed in atmosphere using a CW CO_2 laser with $P_{\rm laser}$ ranging from 1.5 to 13.5 kW/cm^2. The laser spot was focused within 0.2 mm^2 using a hemispherical lens. The CO_2 laser illuminating time was as short as 1 ms. The ablation thickness of SiO_x film was measured by α-step with a resolution of 1 nm. The μ-PL (or μ-PR) of CO_2 laser RTA SiO_x pumped by a HeCd laser at 5 W/cm^2 and 325 nm was detected by a fluorescence spectrophotometer (Jobin Yvon, TRIAX-320). The μ-PR analysis is demonstrated using a similar system with a HeNe laser at wavelength and power of 632.8 nm and 2 mW, respectively. A HRTEM (JEOL, 4000EX TEM) with a point-to-point resolution of 0.17 nm was used to characterize the orientation, lattice constant, size, and density of the precipitated Si nanocrystals in SiO_x film.

Manuscript received March 24, 2006; revised April 4, 2006. This work was supported in part by the National Science Council (NSC) of the Republic of China under Grant NSC 94-2215-E-009-040 and Grant NSC 94-2120-M-002-010. The review of this paper was arranged by Associate Editor F. Terry.

G.-R. Lin is with the Graduate Institute of Electro-Optical Engineering and Department of Electrical Engineering, National Taiwan University, Taipei 106, Taiwan, R.O.C. (e-mail: grlin@ntu.edu.tw).

C.-J. Lin is with the Department of Photonics and Institute of Electro-Optical Engineering, National Chiao Tung University, Hsinchu 300, Taiwan, R.O.C.

L.-J. Chou and Y.-L. Chueh are with the Department of Materials Science and Engineering, National Tsing Hua University, Hsinchu 300, Taiwan, R.O.C.

Digital Object Identifier 10.1109/TNANO.2006.877426

III. Results and Discussion

A. Surface Temperature Evaluation

The surface temperature (T_{surface}) of the SiO_x film under the CO_2 laser RTA process was determined using a previously developed thermal–physical model [11]–[13]. Neglecting the heat transport due to convection, the thermal radiation, and thermal expansion, the absorbed thermal energy per unit volume and per unit time of the SiO_x film annealed using a CO_2 laser with a Gaussian-like power envelope can be described as $g_{\text{laser}}(r,z) = 4P_{\text{laser}}(1-R)\exp(-4r^2/D^2)\exp(-\alpha z)/\pi D^2 d_{\text{absorb}}$ [11], where P_{laser} is the illuminating intensity of the CO_2 laser, R is the optical reflectivity of $R = [(n-1)^2+k^2]/[(n+1)^2+k^2]$, r is the distance to the center of the focused laser spot, D is the beam diameter at 1/e intensity of the Gaussian distribution, α is the optical absorption coefficient of the SiO_x film, ($\alpha = 4\pi k/\lambda$), λ is the laser wavelength, and d_{absorb} is the penetrating depth of the CO_2 laser. The real (n) and imaginary (k) parts of the refractive index of the SiO_x film at the wavelength of 10.6 μm in the room temperature are approximately 2.224 and 0.102, respectively. As a result, the temperature $T(r,z)$ and surface temperature T_{surface} of the SiO_x film are expressed by the following equations [11], [12]:

$$T(r,z) = \frac{g_{\text{Laser}}(r,z)\tau}{\rho C_p} = \frac{4(1-R)}{\rho C_p} \times \frac{P_{\text{Laser}}\tau}{\pi D^2 d_{\text{absorb}}} \times \exp\left(\frac{-4r^2}{D^2}\right) \times \exp(-\alpha|z|) \quad (1)$$

$$T_{\text{surface}}(r) = \frac{4(1-R)}{\rho C_p} \times \frac{P_{\text{Laser}}\tau}{\pi D^2 d_{\text{absorb}}} \times \exp\left(\frac{-4r^2}{D^2}\right) \quad (2)$$

$$\frac{\partial T_{\text{surface}}(r)}{\partial r} = \left(\frac{-4r^2}{D^2}\right) \times \frac{4(1-R)}{\rho C_p} \times \frac{P_{\text{Laser}}\tau}{\pi D^2 d_{\text{absorb}}} \times \exp\left(\frac{-4r^2}{D^2}\right), \quad r \geqq 0 \quad (3)$$

where τ, ρ and C_p are the illuminating time, the density, and the specific heat of the SiO_x film, respectively. The optical absorption coefficient (α), the optical reflectivity (R), the Gaussian beam diameter at 1/e intensity (D), the radial distance (r), the illumination time (τ), the density (ρ), and the specific heat (C_p) of the SiO_x film are set as 1209 cm^{-1}, 0.145, 370 μm, 21 μm, 1 ms, 2800 kg/m^3, and 1270 J/kg/K, respectively. According to these parameters, the simulated T_{surface} of the SiO_x film can be increasing from 130 °C and 3350 °C as the CO_2 laser P_{laser} enlarges from 1.5 to 13.5 kW/cm^2. Therefore, the T_{surface} of the SiO_x film proportional to the CO_2 laser P_{laser} is estimated from (2). For example, the SiO_x surface temperature profile around the annealed zone under illuminating with the P_{laser} of 6 kW/cm^2 is shown in Fig. 1. The surface temperature at the central part of a Gaussian-beam illuminated zone is about 1349 °C. The temperature gradient around the annealed zone of the SiO_x film is also plotted in Fig. 1. Within an illuminating spot of 400 μm diameter, the maximum temperature gradient is only 4.5 °C/μm.

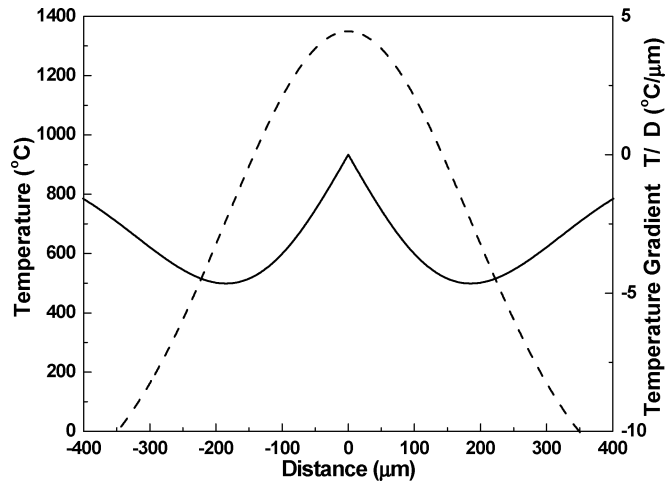

Fig. 1. Surface temperature and temperature gradient in the annealing zone of SiO_x illuminated by CO_2 laser at $P_{\text{laser}} = 6$ kW/cm^2.

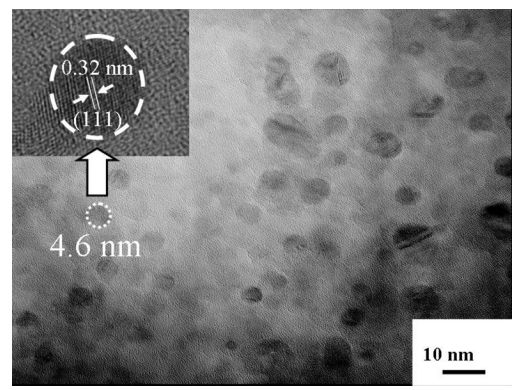

Fig. 2. HRTEM cross-sectional image of the laser RTA SiO_x film by CO_2 laser at $P_{\text{laser}} = 5.8$ kW/cm^2.

B. HRTEM Analysis

As a result, the simulated T_{surface} of the SiO_x film can increase from 130 °C to 3350 °C as the CO_2 laser P_{laser} enlarges from 1.5 to 13.5 kW/cm^2. At $P_{\text{laser}} = 5.8$ kW/cm^2 (or $T_{\text{surface}} = 1285$ °C), the cross-sectional HRTEM image reveals that the diameters of Si nanocrystals precipitated in the SiO_x matrix range from 3 to 8 nm, as shown in Fig. 2. The orientation of Si nanocrystals embedded in the SiO_x film is random, including the (111)-orientation with a lattice spacing of about 0.32 nm, as shown in the inset of Fig. 2. The HRTEM estimated density of the Si nanocrystals in the CO_2 laser RTA SiO_x film at $P_{\text{laser}} = 5.8$ kW/cm^2 is about 4.5×10^{16} cm^{-3}. Similar laser recrystallization was previously demonstrated by using a tightly focused continuous-wave Ar^+ laser ($\lambda = 514.5$ nm) [14], which helps to synthesize Si nanocrystals in the hydrogenated amorphous SiO_x (a-SiO_x : H) film. It was found that the diameter of the Si nanocrystals increases from 2.5 to 12 nm under an extremely high P_{laser} of ranging from 600 kW/cm^2 to 2.6 MW/cm^2. However, the surface damage of the a-SiO_x : H film was also evidenced at such high intensities even with a short irradiating time. A later experiment showed similar results by using a frequency-tripled Nd : YAG laser at wavelength and pulsewidth of 355 nm and 8 ns, respectively [15]. By increasing

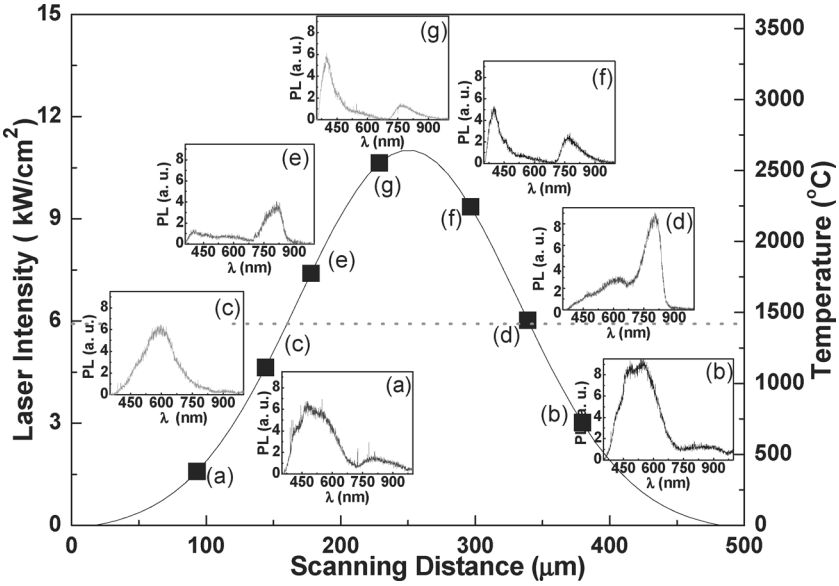

Fig. 3. μ-PL spectra of CO_2 laser annealed SiO_x at different site of the annealed spot area.

the peak energy density of the Nd : YAG laser up to 350 mJ/cm^2, the size of Si nanocrystals can be enlarged to 200 nm. Such a process exhibits a similar surface damage problem, since the peak P_{laser} of 4.4 MW/cm^2 on the sample surface is far beyond the ablation threshold. Gallas *et al.* [16] then observed that the threshold energy density of a 248-nm KrF pulsed excimer laser for annealing SiO_x without any ablation is only 85 mJ/cm^2. Nonetheless, only a few Si nanocrystals can be precipitated in SiO_x under such low P_{laser}, since few laser energies are absorbed and transferred to heat by the SiO_x film with infinitely small absorption coefficient at such short wavelengths (for example, $\alpha < 1 \times 10^{-6}$ cm^{-1} at <532 nm) [13]. In contrast, the CO_2 laser crystallization can precipitate Si nanocrystals at a P_{laser} of at least two orders of magnitude smaller than that required for visible or UV lasers, which simultaneously eliminates the laser-ablation induced surface damage effect. The phase separation between Si and oxygen atoms can be initiated when sufficient energy is absorbed by the SiO_x film; however, the annealing temperature for the precipitation of Si nanocrystals should be higher than 900 °C. Nesheva *et al.* [17] have observed the formation of amorphous Si nanoparticles in films annealed at 700 °C for 1 h. To format the crystallite Si nanocrystals in SiO_x films, a furnace annealing at 1030 °C for 1 h is mandatory, as confirmed by Raman scattering analysis. In addition, Yi *et al.* [18] have also demonstrated that the amorphous Si clusters can be formatted at annealing temperature ranging between 300 °C and 900 °C, but the crystallization of these amorphous Si clusters is only observed by annealing in a nitrogen atmosphere at $>$ 900 °C for 1 h. That is, the annealing temperature of lower than $<$ 900 °C could not activate the crystallization process for the amorphous Si clusters, even if the annealing duration is lengthened. Under CO_2 laser annealing, the surface temperature of the SiO_x film is dependent on the CO_2 laser intensity, the lower CO_2 laser intensity will reduce the surface temperature of the SiO_x film. Our simulation has also interpreted a threshold annealing intensity of 4.5 kW/cm^2, which corresponds to a surface temperature of 1100 °C for initiating the crystallization of the Si nanocrystals. Similarly, the Si nanocrystals are difficult to be precipitated and the size of the Si nanocrystals could not be larger at a lower CO_2 laser intensity even with longer exposure times.

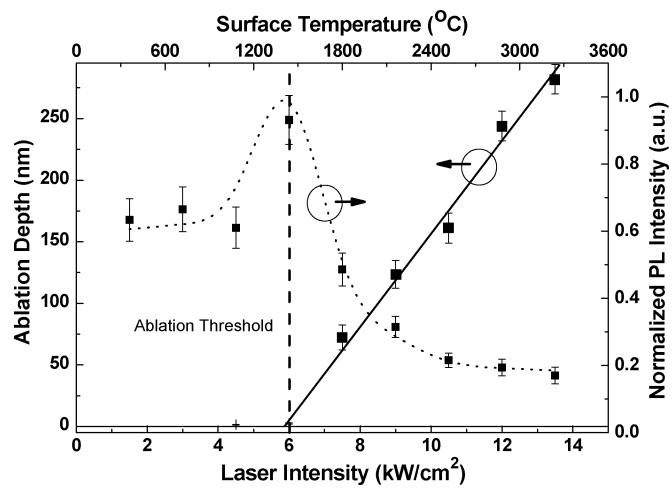

Fig. 4. Laser ablated depth and normalized PL intensity of the laser RTA SiO_x film as a function of P_{laser}.

C. μ-PL and μ-PR Analyses

Subsequently, the μ-PL and μ-PR are employed to characterize the localized optical properties of the CO_2 laser RTA SiO_x film. The power-dependent μ-PL analysis reveals different luminescent features at annealing and ablation regions. The diameter and area of the CO_2 laser annealed zone are 500 μm and 0.2 mm^2, respectively. A tightly focused He–Cd laser beam, with a spot size much smaller than that of the CO_2 laser zone, transversely scans across the CO_2 laser annealed SiO_x sample. In the outer area of the Gaussian laser spot, the SiO_x matrix is not recrystallized and the Si nanocrystal is unable to

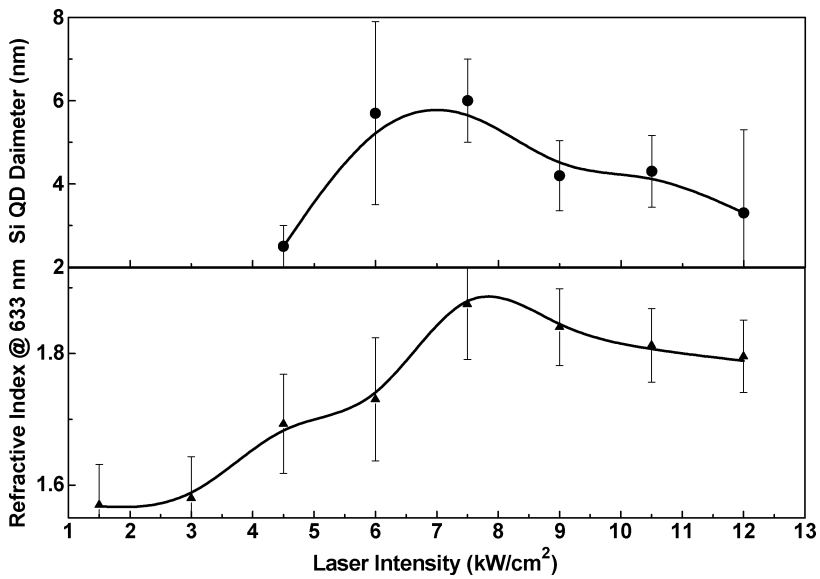

Fig. 5. The size of Si nanocrystal (upper part) and the refractive index of CO_2 laser RTA SiO_x film (lower part) at different laser intensities.

be precipitated, since the P_{laser} as well as the equivalent T_{surface} is relatively low. A broadband blue–green PL contributed by the radiative defects such as E'_δ centers [19] at 520 nm and the neutral oxygen vacancies centers [20] at 455 nm are observed (see Fig. 3). The PL peak red-shifts to 520 nm as P_{laser} slightly increases to 3 kW/cm^2 (equivalent to a surface temperature of 900 °C), indicating a more pronounced activation of the E'_δ defects than the oxygen vacancies (see inset (b) of Fig. 3). Near the central region of the annealing spot, the precipitation of small-size Si nanocrystals (with a size of 0.8–1 nm) is initialized as the PL has further red-shifted to 600–620 nm at $P_{\text{laser}} = 4.5$ kW/cm^2 (or a corresponding surface temperature of 1100 °C). The average size of Si nanocrystals persistently enlarges as the significant PL at 806 nm with spectral width of 106 nm is obtained at $P_{\text{laser}} = 5.8$ kW/cm^2 (see inset (d) of Fig. 3). The maximum PL peak wavelength is observed at 825 nm at $P_{\text{laser}} = 7.5$ kW/cm^2. Nonetheless, the density of Si nanocrystals in SiO_x also decreases at higher annealing laser intensities as the PL intensity at corresponding wavelength is greatly attenuated by an order of magnitude. The effect of P_{laser} on the laser ablation of the SiO_x film clearly shows a linear ablation slope of 35 nm/kW/cm^2 at P_{laser} beyond ablation threshold (6 kW/cm^2), as shown in Fig. 4. The corresponding temperature on the SiO_x surface is up to 1902 °C as P_{laser} becomes > 7.5 kW/cm^2, which has already exceeded over the melting temperature of fused silica. Moreover, a CO_2 laser annealing process at $P_{\text{laser}} > 7.5$ kW/cm^2 not only anneals the SiO_x film and precipitates Si nanocrystals locally, but also leads to an increasing of structural damage related PL at 410 nm by at least one order of magnitude. The SiO_x matrix could be promptly compressed during such a rapid laser ablation procedure, where numerous oxygen-dependent defects such as weak oxygen bond (O-O) [21], oxygen vacancy, and ionized oxygen molecule (O_2^-) [22], [23] with PL wavelengths at 410–455 nm are generated by the damaged bonds of the SiO_2 matrix (see inset (f)–(g) of Fig. 3). Such a phenomenon was never observed in furnace annealed SiO_x film under a similar condition, as the furnace annealing usually causes a gradual recovery on the compressing strain of SiO_2 matrix nearby Si nanocrystals.

The refractive indexes of CO_2 laser RTA SiO_x films measured by μ-PR greatly increase from 1.57 to 1.87 as P_{laser} increases from 1.5 to 7.5 kW/cm^2 (lower part of Fig. 5). The as-grown SiO_x deposited under a N_2O/SiH_4 flow ratio of 6 exhibits comparable refractive index with that reported by Ueno *et al.* [24]. The decrease in the N_2O/SiH_4 flow ratio from 7 to 0.2 leads to an increasing refractive index of SiO_x from 1.48 to 2.1. Such a variation is correlated with the precipitation of Si nanocrystals. At a surface temperature below 600 °C (or $P_{\text{laser}} < 3$ kW/cm^2), the change in refractive index is less than 0.6%, since the precipitation of Si nanocrystals has not yet been initiated. The refractive index of SiO_x reaches a maximum of 1.87 as the surface temperature increases to 1300 °C, while the average diameter of Si nanocrystal is also largest. As evidence, Parakash *et al.* [25] have previously demonstrated that the enlargement of Si nanocrystals can increase the refractive indexes of the furnace-annealed PECVD-grown SiO_x film. The density of the Si nanocrystal is also increased under higher annealing temperature and longer annealing time. A similar refractive index was also observed for the Si-ion-implanted SiO_2 doped by Si nanocrystals with size of 1–3.5 nm [26]. Obviously, the more Si atoms segregate from the SiO_x matrix, the higher density of Si nanocrystals with uniform size can be obtained. From μ-PL, the precipitation of Si nanocrystals in the SiO_x film are initiated at $P_{\text{laser}} > 4.5$ kW/cm^2 (or a corresponding surface temperature of 1100 °C), and the estimated size of Si nanocrystals is increased from 2.8 to 6 nm as P_{laser} increases from 4.5 to 7.5 kW/cm^2, as shown in the upper part of Fig. 5. In contrast, the refractive indexes of the CO_2 annealed SiO_x films slightly decrease from 1.87 to 1.79 as P_{laser} increases from 7.5 to 12 kW/cm^2. Further increasing P_{laser} not only increases the annealing temperature but also activates the segregation of Si atoms and increases the density of the Si nanocrystal concurrently. From this point of view, it is not appropriate to attribute the change in refractive index of SiO_x film only by the

size variation of Si nanocrystals. From HRTEM analysis, it is observed that both the size of the Si nanocrystal is decreased when annealing the SiO_x films at $P_{\text{laser}} > 7.5$ kW/cm^2 due to the reoxidation of the Si nanocrystals. Moreover, the dramatically decreasing intensity of PL emitting from the Si nanocrystals also at higher annealing laser intensities corroborates well with a significant reduction in the density of the Si nanocrystals. This eventually results in a slightly decreasing value of the volume–density product for Si nanocrystals buried in the SiO_x, which evidently elucidates the effect of size and density of Si nanocrystals on the variation in refractive index or absorption coefficient of SiO_x films according to Mie theory [27]. Nonetheless, the effect of the dense oxygen dependent defects on the aforementioned optical constants should also take into account.

IV. Conclusion

In conclusion, the structural and optical properties of the PECVD-grown Si-rich SiO_x film RTA by CO_2 laser are primarily characterized by using μ-PL, μ-PR and HRTEM in this work. The CO_2 laser RTA process performs the *in situ* and localized temperature control of the SiO_x film, which thus facilitates precipitating Si nanocrystals from damaging the nearby devices. The equivalent temperature of the SiO_x surface is increasing from 130 °C to 3350 °C as the CO_2 laser P_{laser} enlarges from 1.5 to 13.5 kW/cm^2. The Si nanocrystals with maximum diameter and density of 8 nm and 4.5×10^{16} cm^{-3}, respectively, can be locally precipitated within the CO_2 laser RTA SiO_x film, giving rise to a near-infrared PL at 790–806 nm. These are obtained at just below ablation-threshold intensity (6 kW/cm^2), which is at least two orders of magnitude smaller than that required for visible or UV lasers. The power-dependent μ-PL analysis indicates that the precipitation of small-size Si nanocrystals is initialized when $P_{\text{laser}} > 4.5$ kW/cm^2 and a maximum PL peak wavelength of 825 nm can be observed at $P_{\text{laser}} = 7.5$ kW/cm^2. Nonetheless, the SiO_x film is ablated with a linear ablation slope of 35 nm/kW/cm^2 at beyond threshold P_{laser} of 6 kW/cm^2. The μ-PR results indicate that the refractive index of the CO_2 laser RTA SiO_x film varies from 1.57 to 1.87 as the P_{laser} increases from 1.5 to 7.5 kW/cm^2. At $P_{\text{laser}} < 3$ kW/cm^2, the change in refractive index is less than 0.6%, since the precipitation of Si nanocrystals has not yet been initiated. The refractive index of SiO_x reaches maximum as the surface temperature increases to 1285 °C, while the average diameter of the Si nanocrystal is also the largest. Annealing at higher intensities not only damages the SiO_x structure, but also constrains the precipitation of Si nanocrystals and decreases the refractive index of the SiO_x. This eventually degrades the near-infrared PL and reduces the refractive index of the CO_2 laser RTA SiO_x film.

References

[1] A. Suzuki and M. Ishihara, "Application of CO_2 laser heating zone drawing and zone annealing to Nylon 6 fibers," *J. Appl. Polym. Sci.*, vol. 83, pp. 1711–1716, 2002.

[2] A. Suzuki and T. Okano, "Zone drawing and zone annealing of Poly(ethyleneterephthalate) microfiber prepared by CO_2 laser thinning," *J. Appl. Polym. Sci.*, vol. 92, pp. 2989–2994, 2004.

[3] Q. He, M. H. Hong, W. M. Huang, T. C. Chong, Y. Q. Fu, and H. J. Du, " CO_2 laser annealing of sputtering deposited NiTi shape memory thin films," *J. Micromech. Microeng.*, vol. 14, pp. 950–956, 2004.

[4] H. C. Pan, C. C. Chou, and H. L. Tsai, "Low-temperature processing of sol-gel derived $La_{0.5}Sr_{0.5}MnO_3$ buffer electrode and $PbZr_{0.52}Ti_{0.48}O_3$ films using CO_2 laser annealing," *Appl. Phys. Lett.*, vol. 83, pp. 3156–3158, 2003.

[5] H. Gleskova, V. V. Ilchenko, V. A. Skryshevsky, and V. I. Strikha, " CO_2-laser annealing of Al/a–Si–H contact," *Czechoslovak J. Phys.*, vol. 43, pp. 169–178, 1993.

[6] V. S. Serbesov, P. A. Atanasov, and R. I. Tomov, "Modification of the properties of HTSC YBCO thin-films on silicon by superfast laser annealing in oxygen with a CW CO_2-laser," *J. Mater. Sci.*, vol. 5, pp. 272–274, 1994.

[7] N. F. Wang, M. P. Houng, and Y. H. Wang, " CO_2 laser annealing on fluorinated silicon oxide films," *Jpn. J. Appl. Phys. Pt. 1*, vol. 38, pp. 5227–5231, 1999.

[8] S. Ono and Y. Masuo, "Crystallization and sintering ofamorphous alumina powder by CO_2 laser irradiation," *J. Ceramic Soc. Jpn.*, vol. 112, pp. 577–580, 2004.

[9] A. F. Maciente, V. R. Mastelaro, A. L. Martinez, A. C. Hernandes, and C. A. C. Carneiro, "Surface crystallization of $\beta - BaB_2O_4$ phase using a CO_2 laser source," *J. Non-Crystal. Solids*, vol. 306, pp. 309–312, 2002.

[10] L. Pavesi, L. Dal Negro, C. Mazzoleni, G. Franzo, and F. Priolo, "Optical gain in silicon nanocrystals," *Nature (Lond.)*, vol. 408, pp. 440–444, 2000.

[11] J. Zhao, J. Sullivan, J. Zayac, and T. D. Bennett, "Structural modification of silica glass by laser scanning," *J. Appl. Phys.*, vol. 95, pp. 5475–5482, 2004.

[12] T. R. Shiu, C. P. Grigoropoulos, D. G. Cahill, and R. Greif, "Mechanism of bump formation on glass substrates during laser texturing," *J. Appl. Phys.*, vol. 86, pp. 1311–1316, 1999.

[13] E. D. Palik, *Handbook of Optical Constants of Solids*. New York: Academic, 1985, pp. 179–182.

[14] M. C. Rossi, S. Salvatori, F. Galluzzi, and G. Conte, "Laser-induced nanocrystalline silicon formation in a-SiO matrices," *Mater. Sci. Eng. B*, vol. 9, pp. 299–302, 2000.

[15] A. Janotta, Y. Dikce, M. Schmidt, C. Eisele, M. Stutzmann, M. Luysberg, and L. Houben, "Light-induced modification of a-SiOx II: Laser crystallization," *J. Appl. Phys.*, vol. 95, pp. 4060–4068, 2004.

[16] B. Gallas, C.-C. Kao, S. Fisson, G. Vuye, J. Rivory, Y. Bernard, and C. Belouet, "Laser annealing of SiOx thin films," *Appl. Surf. Sci.*, vol. 185, pp. 317–320, 2002.

[17] D. Nesheva, C. Raptis, A. Perakis, I. Bineva, Z. Aneva, Z. Levi, S. Alexandrova, and H. Hofmeister, "Raman scattering and photoluminescence from Si nanoparticles in annealed SiOx thin films," *J. Appl. Phys.*, vol. 92, pp. 4678–4683, 2002.

[18] L. X. Yi, J. Heitmann, R. Scholz, and M. Zacharias, "Phase separation of thin SiO layers in amorphous SiO/SiO_2 superlattices during annealing," *J. Phys.: Condens. Matter*, vol. 15, pp. S2887–S2896, 2003.

[19] G.-R. Lin, C. J. Lin, and C. K. Lin, "Defect-enhanced photoconductive response of silicon-implanted borosilicate glass," *Appl. Phys. Lett.*, vol. 85, pp. 935–937, 2004.

[20] H. Nishikawa, R. Nakamura, and J. H. Stathis, "Oxygen-deficient centers and excess Si in buried oxide using photoluminescence spectroscopy," *Phys. Rev. B*, vol. 60, pp. 15910–15918, 1999.

[21] J. C. Cheang-Wong, A. Oliver, J. Roiz, and J. M. Hernanaez, "Optical properties of Ir^{2+}-implanted silica glass," *Nucl. Instrum. Methods Phys. Res. B*, vol. 175, pp. 490–494, 2001.

[22] C. J. Lin and G.-R. Lin, "Defect-enhanced visible electroluminescence of multi-energy silicon-implanted silicon dioxide film," *IEEE J. Quantum Electron.*, vol. 41, no. 3, pp. 441–447, Mar. 2005.

[23] C. Itoh, T. Suzuki, and N. Itoh, "Luminescence and defect formation in undensified and densified amorphous SiO_2," *Phys. Rev. B*, vol. 41, pp. 3794–3799, 1990.

[24] K. Ueno, T. Kikkawa, and K. Tokashiki, "Reactive ion etching of silicon oxynitride formed by plasma-enhanced chemical-vapor-deposition," *J. Vac. Sci. Technol. B*, vol. 13, pp. 1447–1450, 1995.

[25] G. V. Prakash, M. Cazzanelli, Z. Gaburro, L. Pavesi, F. Iacona, G. Franzo, and F. Prilolo, "Linear and nonlinear optical properties of plasma-enhanced chemical-vapor deposition grown silicon nanocrystals," *J. Modern Opt.*, vol. 49, pp. 719–730, 2002.

[26] A. E. Naciri, M. Mansour, L. Johann, J. J. Grob, and C. Eckert, "Correlation between silicon nanocrystalline size effect and spectroscopic ellipsometry responses," *Thin Solid Films*, vol. 455–456, pp. 486–490, 2004.

[27] G. Mie, "Contribution on the optics of turbid media, especially colloidal metallic solutions," *Ann. Phys.*, vol. 25, pp. 377–445, 1908.

Gong-Ru Lin (SM'03) received the Ph.D. degree in electrooptical engineering from National Chiao Tung University, Hsinchu, Taiwan, R.O.C., in 1996.

He is a Professor who directs the laboratory of high-speed photonic systems and measurements with the Department of Photonics and Institute of Electro-Optical Engineering at National Chiao Tung University. He has (co)authored 100 papers in international periodicals and 140 papers in international conferences. His researches include femtosecond fiber lasers, nanocrystallite Si photonics, all-optical data processing, and millimeter-wave photonic phase-locked loops and phase shifters.

Prof. Lin has served as the treasurer of the IEEE Lasers and Electro-Optics Society (LEOS) Taipei Chapter since 2004.

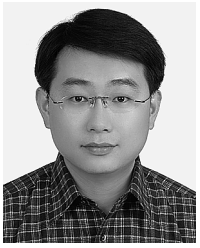

Chun-Jung Lin was born in Taipei, Taiwan, R.O.C., in 1973. He received the B.S. degree in electrical engineering from Feng Chia University, Taichung, Taiwan, in 1998 and the M.S. degree in electrooptic engineering from Tatung University, Taipei, in 2000. He is currently working toward the Ph.D. degree in the Department of Photonics and the Institute of Electro-Optical Engineering at the National Chiao Tung University, Hsinchu, Taiwan.

His research interests are in the design, fabrication, and analysis of nanocrystallite Si materials for light-emitting applications.

Li-Jen Chou, photograph and biography not available at the time of publication.

Yu-Lun Chueh, photograph and biography not available at the time of publication.